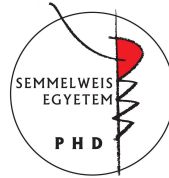


Implementation of In Silico Biomechanical Methods in Spine Surgery Innovations

Ph.D. thesis outline

Péter Endre Éltés M.D.

Semmelweis University
Doctoral School of Clinical Medicine



Supervisor: Áron Lazáry, MD., Ph.D.

Official reviewers:

Lajos Borbás, Ing. Ph.D.

Árpád Viola, MD., Ph.D.

Head of the Final Examination Committee: László Hangody, D.Sc.

Members of the Final Examination Committee:

Gábor Skaliczki, MD., Ph.D.

István Böröcz, MD., Ph.D.

Budapest

2020

1. INTRODUCTION

Emerging patient- focused and holistic treatment methods generated new technological challenges for medicine that resulted in a new discipline, “in silico medicine”. This new approach places the studying of the human body, thus the biomechanics of the musculoskeletal system into a new context. In silico medicine, including finite-element analysis (FEA) based simulation technologies and three-dimensional printing (3DP), plays a crucial role in the realization of individualized treatments and surgeries. 3DP allows the fast, relatively cheap and accessible production of unique complex geometries. The benefit for the patients and clinicians is based on the application of FEA simulations in presurgical planning, and the preparation of surgeons aided by the 3D printed models in case of highly customized procedures.

For new scientific and technological results or methods in the medicine to be widespread, the knowledge of the “end users”– spine surgeons in this case- must be sufficient. An online survey research has been conducted in the AOSpine community assessing the level of knowledge and attitude of spine surgeons about the 3D printing and modeling technologies.

After the global context is defined regarding the 3D technologies, I investigated two surgical methods developed in the National Center For Spinal Disorders (NCSO), Budapest, Hungary, the Percutaneous Cement Discoplasty and the Closed Loop lumbopelvic reconstruction technic after en-block sacrectomy.

I analysed the changes in the spinal canal dimension following percutaneous cement discoplasty (PCD) as this technique provides a segmental stabilizing effect and indirect decompression of the neuronal elements due to the increase of the spinal canal dimensions. Even though the spinal canal is a complex 3D geometry, the common description of its dimensions and the evaluation of the indirect decompression effect are based on 2D parameters. To accurately measure the real, three-dimensional (3D) changes of the spinal canal after PCD procedure, I aimed to develop a generalisable procedure based on patient-specific 3D computational, volumetric measurements.

Lumbopelvic stabilization after sacropelvic tumor resection is challenging as there is no gold standard and relatively high complication rates are reported with all reconstruction strategies. The “en- bloc” resection of a sacral chordoma by performing a total sacrectomy with soft tissue and bony reconstruction and lumbopelvic stabilization can be achieved by the “closed loop” technique. The technique uses a “U” shaped rod which is attached to iliac and transpedicular screws to rebuild the spinopelvic connection. Based on patient-specific 3D geometries derived from CT scans I aimed to develop a generalisable method to investigate the implant construct deformation over 6-year follow-up (FU) for a reconstruction technique.

3D printed technologies aid the preoperative planning, save time in the operating room and provide patient-specific solutions for complex cases through personalized implants. However, the additional costs and time-consuming production of 3D printed physical models with current technologies are hindering its widespread use in hospitals. Therefore, the development of cost effective, sustainable strategies related to clinical application of 3D printing technologies are not only highly desirable but decisive. In my thesis I present a method to compare the geometrical accuracy of two 3D printing technologies used for printing spine physical models. Advantages and disadvantages were weight up in an entry level technology (cost effective, most affordable) with a higher category technology (more precise, more expensive). I also reveal an institutional strategy of the application of 3D printed physical models by presenting a clinical case, in which a model printed with the entry level technology was used in the preoperative planning.

3D geometries from preoperative CT scans in combination of fluoroscopy-based imaging or intraoperative CT scan are used in computer-assisted surgery (CAS) providing a safe and accurate guiding system for the placement of pedicle and lateral mass screws in the spine. In my thesis, I present a case by whom the clinical need for the development of a computer-aided design (CAD) and finite-element analysis (FEA) combined method for affordable spine surgical navigation with 3D printed customized drill guide was raised.

2. OBJECTIVES

The general aim of my PhD work was to investigate the implementation of In Silico Biomechanical Methods in Spine Surgery Innovations.

In the first part of my PhD thesis I pursue to answer the question of what determines the acceptance rate and the factors which stand against the wider spread of the 3D technologies in spine surgery (Eltes et al., 2019). For this I developed and performed a survey-based study among AOSpine members. In the second and third part of my PhD work, I investigated two surgical methods developed in the NCSD the PCD and the Closed Loop lumbopelvic reconstruction technique. In part two I aimed to develop a generalizable procedure based on patient-specific 3D computational, volumetric measurements to evaluate the geometrical change of the spinal canal after PCD treatment. The objective of part three is to develop a generalizable method based on patient-specific 3D geometries derived from CT scans in order to explore the implant construct deformation over 6-year follow-up (FU) for a patient who underwent sacrectomy and Closed Loop reconstruction technique was used for lumbopelvic reconstruction.

The global perspective on the attitude of the spine surgeons towards the application of 3D technologies given by the survey study raises the need for strategies to implement 3D printing and FEA in the clinical environment in an affordable way.

Part four of my thesis addresses the need for the application of affordable 3D printing technology for spine physical models. Here I developed an institutional strategy for application of the 3D printed physical models. Part five of my thesis focuses on the clinical need for the development of computer-aided design (CAD) and finite-element analysis (FEA) combined method for affordable spine surgical navigation with a 3D printed customized drill guide to allow safe pedicle screw insertion in challenging situations.

3. MATERIALS AND METHODS

3.1. PART I. Clinical needs finding for 3D technologies, a survey of AOSpine members

In October 2016, an online survey was sent out a single time to all AOSpine members on the mailing list. The questionnaire included 21 multiple choice or ordinal scale questions, being divided on thematic chapters (one page each) as follows: (I.) question I/1-6 we collected demographic data of the respondents; (II.) questions II/1-3 focused on the personal use of 3D printed or virtual 3D models; (III.) questions III/1-5 focused on the use and attitude towards 3D technologies in surgical navigation; (IV.) questions IV/1-5 investigated the advanced manufactured (3DP) and patient-specific implants; in chapter (V.) we ask questions V/1-2 about the future and limitations of 3D technologies. The influence of geographical location (AOSpine region), spine surgical practice, experience, etc. on the acceptance score was analyzed statistically. Participants of our survey were grouped based on the HDI (Human Development Index) of their country of residence and survey results were analyzed in the context of this parameter too.

3.2. PART II. A novel method for patient-specific computational analysis of three-dimensional changes in spinal canal dimensions after percutaneous cement discoplasty

3.2.1. Clinical cohort and CT scan acquisition

We performed a retrospective analysis of prospectively collected data. The cohort consisted of 10 patients (74 ± 7.7 years old), who underwent primary single or multilevel percutaneous cement discoplasty (16 motion segments in total) at tertiary care spine referral centre. Preoperative (preop), and postoperative (postop) 6-month follow-up data were collected and analysed using patient reported outcome questionnaires; Oswestry Disability Index (ODI) and with visual analogue scale (VAS) for leg pain (LP) and low back pain (LBP). Quantitative Computed Tomography (QCT) scans were performed pre- and postoperatively.

3.2.2. Definition of pre- and postop motion segments' 3D geometry

In order to establish the 3D vertebral geometry of the pre- and postop motion segments and the injected polymethyl methacrylate (PMMA) geometry, a segmentation process was performed on the 2D CT images. For this, the thresholding

algorithm and manual segmentation tools (erase, paint, fill etc.) in Mimics® image analysis software (Mimics Research, Mimics Innovation Suite v21.0, Materialise, Leuven, Belgium) were used. To evaluate the accuracy of the segmentation process, we calculated the Dice Similarity Index (DSI).

3.2.3. Alignment of the motion segments' geometry

To detect the PCD induced changes in the postop motion segment, the pre- and postop vertebral geometries were aligned in the same coordinate system. For this, preop 3D data sets were transposed into the same coordinate system with the postoperative data. Pre- and postop caudal vertebra surface mesh models of the treated motion segments were used as reference geometry. Control points based rigid registration algorithm was used via Mimics® software. To evaluate the accuracy of the registration and alignment procedure the Hausdorff Distance (HD) values were calculated at the vertices of the triangulated surface meshes.

3.2.4. Measurement of the neuroforaminal 3D geometry

After alignment, the change in spinal canal geometry, induced by the injected PMMA in the intervertebral space during the PCD procedure, was defined for the two datasets (aligned by I_1 , I_2). A measurement cylinder was created using Mimics® software, analyse module. The cylinder was inserted in the virtual coronal axis of the neuroforamen (coronal plane). Its length was defined at 90 mm, while the radius of the cylinder was set by the investigators uniquely in each patient and segment in a way to fill the neuroforamen's volumes and the central canal in pre and postop 3D geometries of the motion segments. The overlapping volumes between the cylinder and the motion segment 3D geometry were subtracted. The change in the subtracted cylinder volumes represents the spinal canal dimension $V_{\text{preop}} = 3D \text{ Cylinder} - (3D \text{ Cylinder} - \text{Preop } 3D \text{ motion segment})$, and $V_{\text{postop}} = 3D \text{ Cylinder} - (3D \text{ Cylinder} - \text{Postop } 3D \text{ motion segment})$. The change in the subtracted cylinder volumes represents the indirect decompression effect of the surgical procedure.

3.2.5. PMMA geometry visualisation and thickness measurement

The 3D geometry of the intervertebral PMMA for the 16 treated motion segments were defined during the segmentation process, by a uniformly remeshed triangulated surface mesh. The surface mesh defines the geometry and determines the surface and the volume of the object. In 3-matic® software (Mimics Innovation Suite v21.0, Materialise, Leuven, Belgium) thickness measurement was performed and visualised using contour plots.

3.3. PART III. A novel computational method to assess implant deformation and to map bony fusion in a lumbopelvic reconstruction after en block sacrectomy

3.3.1. Clinical Case

The 42-year-old male patient's case and surgery was presented in the European Spine Journal, *Open Operating Theatre* (OOT) section. Total en bloc

sacrectomy combined with soft tissue and bony reconstruction together with lumbopelvic stabilization (closed loop technique) was performed to remove the tumor.

3.3.2. Postoperative Computed Tomography scan acquisition

We performed a retrospective analysis of retrospectively collected postoperative (postop) Computed Tomography (CT) data. The data set consisted of 12 CT covering a 6-year follow-up period (FU).

3.3.3. Gait evaluation after total sacrectomy

During the surgery the lumbosacral intervertebral disc was resected, and the dural sac was cut through immediately below the L5 origins. Bilaterally the cranial and ventral ligaments of the SI joints and the nerve roots (bilaterally below the S1) were cut through at the lateral aspect of the tumor. However, the patient was able to walk with crutches at 3- month (m) FU, and without any assisting device at 12m FU. To quantify and evaluate the gait of the patient at 6 years FU a gait analysis was performed. Gait data was acquired while the patient walked along a straight path at a self-selected speed. The subject was fitted with a full body VICON plug-in-gait marker setup. Three-dimensional kinematic data was recorded using a 6-camera system (MXT40, VICON, UK). Kinetic data was acquired using one force platform (AMTI OR6, USA) mounted halfway along the path. Lower limb kinematics and kinetics were calculated using NEXUS (VICON, UK) and compared to normative data.

3.3.4. Image processing, 3D geometry definition

In order to define the deformation of the Closed Loop implant construct we defined the construct 3D geometry and arbitrary the left iliac bone 3D geometry in every CT data set. We considered the iliac bone geometry constant, however at the fusion site after the alignment a symmetric geometry reduction was performed by a cube subtraction. To exclude the geometrical difference, the same subtraction was performed for all geometries at the Ischial ramus, where the last axial CT slice ended for the first post op scan (for the rest all the pelvis was covered in the scan). Segmentation process was performed on the 2D CT images. From the segmented masks, a triangulated surface mesh was automatically generated for the iliac bone and for the implant construct. To evaluate the accuracy of the segmentation process, we calculated the Dice Similarity Index (DSI).

3.3.5. Alignment of the implant construct geometries

To determine the implant deformation, the 12 segmented (I_i) implant geometry with the iliac bone were aligned in the same coordinate system (I =investigator). The first postop CT scan based left iliac bone was used as the reference geometry. A control points based rigid registration algorithm was used via Mimics[®] software. To evaluate the accuracy of the registration and alignment procedure the Hausdorff Distance (HD) was measured with the MeshLab1.3.2 software Metro tool algorithm at the level of the aligned Iliac bones. The alignment of

the 12 geometry was calculated by I_1 , and the HD measurements were determined from the second postop CT scan to the last 12th scan compared to the first postop scan-based geometry. After registration of the iliac bones the trans iliac screws body's geometry overlapped. The axis of the iliac screws were considered to be collinear and coincident. To test this hypothesis, HD values were calculated for the screw's bodies by comparing the geometries to the first postop CT scan geometry after the alignment.

3.3.6. Implant deformity measurements

The implant construct geometry was considered a tubular structure and the centreline of the geometry was defined with the Mimics Software. A „mobile” point corresponding to the L.II right pedicle screw tip and a fix point was selected in the centreline corresponding to the tip of the caudal iliac screw. The distances between the point were measured in three anatomical planes using 3-matic® software (Mimics Innovation Suite v21.0, Materialise, Leuven, Belgium). The segmentation of the implant construct, the centreline definition and the distance measurement in the three planes was performed by three investigators (I_1, I_2, I_3) at two different time points (T_1, T_2). For the repeatability and reliability test of the measurements from the X_d (coronal plane), Y_d (axial plane), Z_d (sagittal plane) the three-dimensional distance $3D_d$ was calculated.

3.3.7. Mapping of the bony fusion

In every CT scan, the same region of interest (midplane between the right L4 and L5 pedicle screw) was selected from a single axial slice. The bone tissue was segmented based on thresholding algorithm, to determine the outer boundary of the bony element (left and right iliac bone, and L4 vertebra). The mask internal part was filled, and a homogenous mask was created, from this mask a voxel-based FE mesh was created with the Mimics Software. From the institutional PACS database QCT scans were selected with the same acquisition protocol and machine. The date of the scans were selected to be in the same month as the postop CT scans. The subjects also had to have similar body mass indexes ($BMI=28\pm 2$) as the presented patient ($BMI=28$). The Hounsfield Units values of the QCT images were converted into BMD equivalent values by using a densitometric calibration obtained with an inline phantom (HitachiPresto, Hitachi Medical Corporation, Tokyo, Japan) with five cylindrical insertion with known mean equivalent BMD values (0, 0.5, 0.1, 0.15, and 0.2g/cm^3). Based on the 12 QCT a mean conversion curve was defined and assumed to be linear according to studies from literature. In the voxel-based FE mesh every element was coded with 10 different colour code corresponding to the BMD values. The distribution of the FE mesh voxel element over the FU was analysed. The volume of the BMD categories were calculated (voxel dimension*number of elements) and visualised using a 3D surface plot created with SigmaPlot 12 (SSI, San Jose, California, United States).

3.4. PART IV. Application of 3D printing in Spine care

3.4.1. Definition of the 3D geometry

A CT scan of a lumbar fourth (L.IV) vertebra of a 25-year-old patient was selected. The vertebra of our interest and the neighboring segments were not affected by any musculoskeletal pathology. In order to define the 3D geometry, we performed thresholding and manual segmentation in 3D Slicer 4.1.1 To evaluate the accuracy of the segmentation process, we calculated the Dice Similarity Index (DSI) with 3D Slicer DiceComputation tool. DSI value of the segmentation process was 0.96 indicating a high accuracy.

3.4.2 3D printing

The segmented geometry was converted to STereoLithography (STL) format using the “ModelMaker” module of 3D Slicer. Inspection and correction of the 3D geometry was conducted with MeshLab1.3.2 software, and the following adjustments were made on the triangulated surface mesh: (1) isolated pieces were considered artefacts and therefore, were removed; (2) duplicate edges and faces, that resulted from unification were deleted; (3) universal remeshing with contour preservation. A final vertebra model (FVM) was built from 8024 vertices and 16048 triangulated faces. The FVM was printed with the following two 3D printing technologies: (1) Fused Deposition Modelling (FDM) device (Dimension 1200es 3D Printer; Stratasys, Israel) in which a thin filament of plastic (ABSplus in ivory) is melted in an extruding head, which is then deposited to build the desired shape, slice by slice, on a moving platform. During the printing all the significantly protruding parts are supported by a concurrently printed scaffold (printed from a water-soluble plastic; Soluble Support Technology, SST). The internal grid structure of the model is automatically generated. The building size of the machine is 254 x 254 x 305 mm and operates with a layer thickness of 0.330-0.254 mm. (2) The Digital Light Processing (DLP) device (VOXEL L 3D Printer; Do3D, Hungary) polymerizes selectively illuminated planes of the model, slice by slice. The DLP uses a model material Voxeltek White Resin (photo-polymer, acrylic based), and a light emitting diode (LED; with ultraviolet spectrum) as a light source. Upon selective illumination, the model material becomes polymerized and solid. The internal structure of the printed vertebra is empty. The building size of the machine is 125 x 65 x 65 mm, the wall thickness for the FVM was set to 1.2 mm, the printer operates with a layer thickness of 0.1-0.025 mm.

3.4.4. Comparison of the 3D physical models printed with FDM or DLP

The FDM and the DLP printed models were scanned (ScanBox 3D scanner; Smart Optics Sensortechnik GmbH, Bochum, Germany) in two measurement sessions and in two orientations. The measurement field was 80x60x85 mm with a resolution of 0.006 mm (ISO 12836). We created FDM-sup and DLP-sup two-point clouds (sup=superior, inf=inferior) and FDM-inf and DLP-inf point clouds. Based on these

point clouds the scanner driving software created triangulated surface mesh models. The models were then exported in STL format.

Following, alignment and rigid surface registration were performed. FDM-sup, DLP-sup, FDM-inf and DLP-inf 3D data sets were transposed into the same coordinate system by surface registration, in order to align their overlapping components with the segmented vertebra surface mesh model (FVM), used as reference geometry. We used MeshLab1.3.2 software Align Tool for the point based rigid registration process. Eight symmetrical (left-right sides, 4-4) and two asymmetrical control points were selected from the superior and inferior region of the reference FVM and from the aligned geometry, respectively. The registration was performed by the two investigators (I_1 , I_2) and at two different time points (T_1 , T_2).

To evaluate the accuracy of the registration and alignment procedure the Hausdorff Distance (HD) was measured with the MeshLab1.3.2 software Metro Tool algorithm. Because the values not only indicate the precision of the printing technology, but also the precision of the surface registration. This process was conducted by two investigators (I_1 , I_2) and at two different time points (T_1 , T_2). The HD values were calculated at the vertices of the triangulated surface meshes.

In order to measure Surface Roughness (SR), two symmetrical rectangular surface areas from the superior endplates and from the right superior part of the pedicles of the aligned (I_1T_1) FDM-sup and DLP-sup meshes were determined and separated as regions of interest (ROI) with Autodesk ReMake and Autodesk Meshmixer 3.1 software. The selected and isolated ROIs were exported in STL format, and the surface roughness was then quantified with CloudCompare v2.6.0 software. For each point (vertices of the triangulated surface mesh), the roughness value represents the distance between the point of interest and the best fitting plane, which is computed from its nearest neighbours within a defined kernel. The kernel size equals with the radius (mm) of a sphere centered on each point.

3.4.5 Application of 3D printed physical models in surgical planning

An FDM model was used for planning the trajectory of transpedicular screw insertion in case of a 12-year-old patient suffering from congenital scoliosis caused by an L.I hemivertebra. A pre-operative CT scan, with 1.25 mm slice thickness, was performed from the lower part of Th.XI vertebra to the upper part of L.III vertebra. To fulfil patient data protection, de-identification of the DICOM data was performed. The vertebrae from the anatomical region of interest were segmented with 3D Slicer 4.1.1 as described in case of the FVM, and a model including Th.XI-L.III vertebrae was created. The segmented volumes were converted to STL using the module ModelMaker option. The model was then printed with FDM technology and was used for planning the trajectory of the screw insertion at the Th.XII and L.I levels.

3.4.6 3D data integration in the clinical communication

The virtual model used in the clinical case was imported in STL format to MeshLab1.3.2 and subsequently saved as a Universal 3D File (U3D). A 3D Portable Document Format (3DPDF) file, containing the U3D mesh, was created using Adobe Acrobat (version 10 Pro Extended) 3D tools with default Activation Settings and assignment of a Poster Image from default view. The 3DPDF file was incorporated in our institutional web browser-based SQL database (Oracle Database 12c) which is accessible by clinicians from any institutional desktop PC or mobile device.

3.5. PART V. Affordable patient-specific surgical navigation

3.5.1. Clinical Case

A 38 year old patient underwent multiple spine surgeries at the L.V-S.I level over 5 year period with trans foraminal interbody fusion (TLIF). During the last surgery implant removal and S.I left side nerve root decompression was performed and 6 months after the patient was referred to our institution. The patient manifested mechanical low back pain, with no sign of sensorimotor deficit. The imaging at the admission showed a broken S.I left side pedicle screw, and a non-union in the L.V-S.I intervertebral space. Refusion surgery was decided, however the broken screw caused a geometrical and technical difficulty for new screw insertion.

3.5.2 Patient specific 3D geometry definition

For the study Quantitative Computed Tomography (QCT) scans were used. The thresholding algorithm and manual segmentation tools (erase, paint, fill etc.) in Mimics image analysis software (Mimics Research, Mimics Innovation Suite v21.0, Materialise, Leuven, Belgium) were used to define the sacrum and the broken screw geometry. The resulting masks (group of voxels) were homogeneously filled by preserving the outer contour of the geometrical border in 2D. From the mask, a triangulated surface mesh was automatically generated.

3.5.3. Surgical planning and FE model generation

A 6.5 diameter and 45 length Medtronic Legacy polyaxial pedicle screw was scanned using a ScanBox 3D scanner (Smart Optics Sensortechnik GmbH, Bochum, Germany). The model of the screw was reconstructed and modified (from polyaxial to monoaxial head) in Autodesk Fusion 360 (Autodesk Inc., California, U.S.A.) and in 3-matic (Mimics Research, Mimics Innovation Suite v21.0, Materialise, Leuven, Belgium) software. The triangulated surface mesh of the screw model was uniformly remeshed. The screw model was virtually inserted in the 3D model of the patient sacrum in two position (convergent S1, divergent ALA) using the Mimics software STL import tool by taking in account and overcoming the broken screw geometry caused difficulty. Two Non-Manifold assembly was created in Mimics software containing the broken screw, the implanted screw and sacrum for the S.I and ALA position. The assembly was exported to 3-matic software where 9-9 FE mesh were

generated for both implantation scenarios (S1, ALA). Adaptive meshing protocol was used for the volume mesh creation with 10 node tetrahedra elements, the maximum edge length of the meshing process corresponded with the initial edge length of the sacrum surface mesh. The material property assignment for element representing the sacral bone tissue was done in two steps. In the first step conversion of the HU (*Hounsfield*) values to the BMD values from the in-line phantom was performed, the conversion curve was assumed to be linear according to studies from literature. In the second step bone tissue was assumed to be isotropic and linearly elastic with a Poisson's ratio of 0.3. Conversion curve between the density and the elastic modulus of bone was based on the correlation established by Kopperdahl et al. The FE models were exported to Abaqus/CAEv11 (Dassault Systemes, Simulia Corp, Providence, RI, U.S.A). For the broken and the inserted pedicle screw the material properties were defined as follows: Poisson's ratio of 0.3, elastic modulus 114000 MPa. The finite element model was subjected to a static 500 N tensile load applied to the screw head and it was fixed at the S1 endplate and the lower 1/3 of the sacrum.

3.5.4. Navigation template design, manufacturing and accuracy evaluation

The virtually inserted screw axis and the individual geometry, the surface of the cranial /dorsal part of the sacrum was the basis for the guide design. In 3-matic software the two-screw insertion axis and surface for the guide/sacrum contact was defined based on the STL assembly (broken screw, inserted implant, sacrum). The contact surface and the axis were exported to Autodesk Fusion 360 CAD (Computer Aided Design) software where the design process was finalised. The manufacturing of the guide was carried out in two steps. First the virtual model of guide was printed with masked stereolithography (MSLA) technology-based 3D printing machine (VOXEL L 3D Printer; Parameters: building size: 125 x 65 x 65 mm, layer thickness: 0.05 mm; Material: Voxeltek Cast Resin; Do3D, Hungary). The used photopolymer design has the advantage that it can be used as pattern for investment casting. The model finally was produced in dental technical laboratory via investment casting (Hexacast induction centrifugal casting machine; parameters: start torque: 0-21 Nm, maximum melting mass: 100 g, max heating: 1750 °C, dimensions (width x height x depth): 660 x 390 x 645 mm; Material CoCr; PiDental, Hungary) from *cobalt-chrome*. The accuracy of the casted part was tested via 3D scanning and compared to the 3D printed model. The point clouds resulted from the scanning were aligned and compared in 3-matic software with the part comparison module.

The accuracy of the guide was tested on a patient-specific sacrum physical model 3D printed with Fused Deposition Modelling technology-based machine (Dimension 1200es 3D Printer; Parameters: building size 254 x 254 x 305 mm, layer thickness 0.330-0.254 mm; Material: ABSplus/ivory; Stratasys, Israel). The drill guide was placed on the FDM model, a cylinder inlet was connected to the guide to support

the drill bit and the drilling of the model was performed according to S1 and ALA position. The Guide was removed and two CT scan was performed with the S1 and ALA positioned drill bit about the sacrum model. The CT scan images were imported to Mimics software where the segmentation (Thresholding) and 3D reconstruction of the patient-specific FDM model geometry and drill bit was performed. The models were registered to the initial sacrum geometry derived from the QCT via point based rigid registration by selecting anatomical landmarks in the caudal part of the sacrum. This step was followed by an automatic global registration inside the 3-matic software. The registration accuracy was measured with the part comparison module of the 3-matic software. The centreline for the drill bit 3D geometry was defined and an analytical primitive (cylinder with 2.5mm diameter was fitted) to define the drilling axis.

4.RESULTS

4.1. PART I. Attitude of spine surgeons towards the application of 3D technologies

Two hundred eighty-three AOSpine members from six AO regions completed the online survey. Most responders were from Europe (N=101, 35.7%). The study population was grouped into three subgroups based on the HDI of the country of the participants. More than half of the subjects (56.0%) have been from a very high HDI country while 30.5% of the responders have come from a country with high HDI and 13.5% from a country with medium HDI. None of the responders were from the low HDI group. Regarding the specialties, 83.7% of the surgeons treat degenerative cases, 50.4% of them have trauma and 39.4% have deformity practice. Out of the responders 27.7% operate on spinal tumors. The majority of the study population has had an experience of 3 to 10 years in spine surgery (33.5%). Regarding the experience 26.7% had 10 to 20 years, while 23.5% have been more experienced surgeons (more than 20 years in spine surgery). Young surgeons (0 to 3 years' experience) represented the 16.4% of the study population.

Seventeen percent of the participants have not had any specific knowledge about the 3D technologies, while a similar rate of the subjects (18%) had already used these techniques. Only 7.1% of the clinicians use regularly 3D virtual or printed models for education or demonstration, while 46.1% of the surgeons have never used them. 3D models can play a significant role in the surgical planning or in the development process of a new surgical method, but 61% of the respondents have never used such a model for that purpose. More than half of the study participants (55%) used some type of navigation in their surgical practice and the rate of regular or occasional users of 3D printed navigation guides was 1.8% and 4.6%, respectively. The claim for a specific, unique surgical instrument has been quite high in the survey population (28% of the surgeons would frequently need such a tool while 56.4% of

them would occasionally need a unique, individually manufactured instrument). Implants manufactured by an advanced technique (e.g. 3DP) are regularly used by a minority of the surgeons (3.2%) and most of them (81.1%) have never used such a spinal implant. About forty percent (40.5%) of the responders have thought that these implants have got a possible advantage in challenging surgeries (e.g. tumor resections, special anatomical variations) and in individual, complex cases where patient-specific implants would be required.

Over half of the spine surgeon community believed that 3D technologies are a promising choice (42%) or will play a revolutionary (12.1%) role, based on the responses related to question V/1. However, 43.8% of the respondents consider it as an option with limited applications in individual cases.

Answers to multiple choice questions revealed that most of the subjects, regardless of the AO region believed costs, lack of access and insufficient knowledge/expertise are limiting the frequent use of 3D technology in clinical/educational practice. In Latin America, Middle- East and Asia- Pacific the high purchasing and maintenance cost, whereas in Europe the high purchasing price and complicated usage, were considered as the main limiting factors. The answers of North Americans point to the redundancy of these 3D navigational technologies in their praxis among the high costs.

4.2. PART II. Investigation of a surgical technique using 3D methods

4.2.1 Evaluation of the segmentation procedure

To evaluate the accuracy of our segmentation process we used the DSI for 6 randomly selected and postoperative geometries. The obtained DSI values for both pre- and postoperative geometries were very high and showed negligible variance, indicating a high accuracy of our segmentation method for all segmented geometries.

Next, for assessing the injected PMMA cement geometries we first evaluated the PMMA geometry distribution over the caudal vertebra endplate of the motion segments visually in 3D in the same view. Because the degenerative processes are not only age dependent, but also depend on the musculoskeletal status of each patient, the features of intervertebral disc degeneration will be widely different. Accordingly, we found that the injected volumes are arranged patient-specifically to widely differing 3D shapes. Because of this large variance, the selection of representative volumes randomly is less likely; therefore, we chose to validate the segmentation process on all injected PMMA volumes instead. We calculated the DSI as above for the 16 segmented geometries. Again, the DSI values were very high for all segmented geometries demonstrating the precision of our segmentation method also in case of the injected PMMA geometries.

4.2.2. Motion segments alignment evaluation

Having confirmed the precision of our segmentation process, as a next step we evaluated the accuracy of the alignment of the pre-and postop motion segments by measuring HD values. The same processes were performed by two investigators (I_1 and I_2). The HD values represent the maximal distance between two corresponding points (vertex) of the respective registered surface meshes. We obtained a mean HD value of 0.43 ± 0.19 mm for the first investigator (I_1), and 0.54 ± 0.16 mm for the second investigator (I_2). These values are considered by the field to be indicative of adequate fitting. To obtain a detailed view on the precision of our alignment we created cumulative probability plots for the measured HD values for both investigators. We found that the maximal distance between the registered pre- and postop 3D geometries were almost always (90%) smaller than 2 mm, and ~70% of the values were smaller than 1 mm. These measurements confirm the accuracy of registration/alignment methods. Consequently, the calculation of volumetric changes of the spinal canal, are expected to be similarly precise.

4.2.3. PCD induced indirect decompression volumetric measurement

We measured the induced modification by defining the spinal canal geometry pre-and postop and calculating the volumetric change. For this, we created measurement cylinders patient-specifically overlapping each preop and postop 3D geometries with impressions of the respective vertebral body, pedicles, facets and vertebral arches (see Materials and Methods Section). We then quantified the indirect decompression effect as the subtracted volumes ΔV ($\Delta V = V_{\text{postop}} - V_{\text{preop}}$). To test the accuracy and reproducibility of these measurements we involved two investigators (I_1 vs I_2) who performed the same procedures at two time points (T_1 vs T_2). Our data indicate high accuracy and reproducibility of the volumetric change measurements. We then, determined the actual volumetric change (ΔV) of the spinal canal in the PCD-treated motion segments as $(I_1T_1+I_1T_2+I_2T_1+I_2T_2)/4$. The observed geometrical change (mean=2266.50, SD=1172.19, n=16) between the preop and postop measurement cylinder volumes demonstrates significant difference (V_{postop} vs V_{preop} , $p < 0.0004$, Paired Wilcoxon signed rank test), meaning that PCD caused a significant increase of the volume of the spinal canal.

4.2.4. PMMA geometry effect on the volumetric change (ΔV) of the spinal canal

We next tested how the geometry of the injected PMMA relates to the observed volumetric change. We found significant, strong and positive correlation between the volume of the injected PMMA and the ΔV of the spinal canal (*correlation coefficient* ($\rho=0.762$, $p=0.001$)). The surface area of the discoplasty showed a significant, strong and positive correlation ($\rho=0.668$, $p=0.005$,) the volumetric change of the spinal canal. A significant and moderate, negative correlation ($\rho= -0.535$, $p=0.033$) was found between the PMMA surface-volume ratio (SF:V) and the

volumetric change of the spinal canal. These data indicate that the volume and surface area of the injected PMMA are the most predictive in regard to the extent of the expected indirect spinal decompression.

4.2.5. Clinical outcome

To test the clinical effect of the indirect decompression we used the patient reported outcome questionnaires; Oswestry Disability Index (ODI) and visual analogue scale (VAS) for leg pain (LP) and low back pain (LBP). The ODI and LP, LBP significantly decreased 6 months after the PCD procedure ($p=0.013$; $p=0.036$; $p=0.015$); respectively, and as such reflecting significant improvement in our patients' pain intensity after PCD procedure. In order to find a predictive measure of clinical improvement we analysed the association of the volumetric change of the spinal canal and ODI, LP and LBP. We found only weak, negative, but non-significant correlation between the change of the ODI and ΔV ($\rho=-0.321$, $p=0.365$), indicating clinical improvement regardless of the indirect decompression volume. However, the correlation between the change of the LP, LBP and ΔV ($\rho=0.772$, $p=0.009$; $\rho=0.693$, $p=0.026$, respectively), was significant, strong and positive. This indicates a volume dependent amelioration of patient symptoms, with a higher injected volume resulting in better patient outcome.

4.3. PART III. Investigation of the Closed Loop lumbo-sacral reconstruction technique using 3D methods

4.3.1. Locomotor biomechanics

The patient was able to walk independently with minor gait alterations to compensate lost neural functions. The gait was slow and asymmetric with more support on the left side. Joint mobility was close to the normative data in all joints, distally in particular. A forward leaning of 20° was seen at the level of the pelvis and trunk throughout the gait cycle. Adduction moments increased at the hip on both sides while joint moments decreased at the knee. Joint power analysis showed a decrease in propulsion power at the hip and ankle.

4.3.2. Evaluation of the segmentation procedure

To evaluate the accuracy of our segmentation process we used the DSI for the 12 CT scan-based implant construct and left iliac bone geometry. The obtained DSI values for the implant construct geometries were very high 0.97 ± 0.02 ($n=12$) as well as for the iliac bone 0.96 ± 0.05 ($n = 12$) and showed negligible variance, indicating a high accuracy of our segmentation method for all segmented geometries.

4.3.3. Alignment evaluation

Having confirmed the precision of our segmentation process, we next evaluated the accuracy of the alignment of the iliac bones to the first postop iliac bone geometry by measuring HD values. We obtained a mean HD value of 0.63 ± 0.14 mm. The HD was determined for the iliac screw bodies by comparing to the first postop

geometry and resulted in a mean value of 0.95 ± 0.10 mm. These values are considered by the professional field to be indicative of adequate fitting. After the iliac bone alignment in order to demonstrate the colinear and coincident position of the iliac screw axis, we visualised the geometric overlap of the iliac screws body's in. The figure demonstrates that the screw body does not deform or change its position in the new common coordinate system. Theoretically any point in this two-screw body geometry can be used as a reference point in a measurement process.

4.3.4. Implant deformation

We defined the implant deformation by measuring the distance in the three planes between the right L.II pedicle screw tip and the left caudal iliac screw tip. The measurements were performed by three investigators at two different time points (I_1, I_2, I_3, T_1, T_2). The mean change in the dimensions compared to the first post op CT was $\Delta X_d = 7.27 \pm 2.80$ mm for the frontal plane, $\Delta Y_d = 8.24 \pm 2.51$ mm for the coronal plane, $\Delta Z_d = 10.15 \pm 2.97$ mm for the sagittal plane. To test the accuracy and reproducibility of these measurements we performed inter- and intrarater reliability test by calculating the intraclass correlation coefficient (ICC) based on the $3D_d$ values. The implant construct deformation can be registered in the anatomical planes over the postop follow up period, however we have found only in the sagittal plane a significant, negative and strong correlation between the Z_d and the number of days after surgery ($\rho = -0.664$, $p = 0.018$). This result demonstrates the forward bending tendency of the construct.

4.3.5. BMD mapping at the fusion site

The bone material density distribution in the region of interest for the fusion process was measured over the follow up period. The colour map captures the bone remodelling process in the ROI. After the second year FU a solid fusion was detected between the lumbar spine L.IV-V vertebra and the two iliac bones, however due to the cyclical loading the bone remodelling represented by the change in the element distribution in the colour coded BMD categories still continues.

4.4. PART IV. Integration of the 3D printed physical models in spine care

4.4.1 Comparison of the FDM and DLP 3D printing technologies

Geometrical differences between the surface meshes printed by the two 3D printing methods are represented by the calculated the Hausdorff Distance (HD) values between the aligned surfaces (FDM-sup, FDM-inf, DLP-sup, DLP-inf) and the FVM. The distribution of the HD values along the vertebral surface meshes provides evidence for high accuracy. However, 'critical points' with higher HD values are revealed: the vertebral endplate in case of the FDM technique (superior surface: I_1T_2 , I_2T_2 ; inferior: I_1T_1); the spinous process and the inferior articular processes in case of the DLP technology. The fact that, these higher HD values are not present in all segmentation processes (investigators and time points), indicates that it is probably a

registration error and not a flaw of the printing technologies. The distribution of the HD values were indeed dependent on the investigators and the measurement time point (I_1 vs I_2 : FDM sup, FDM inf, DLP sup, DLP inf, Two-sample Kolmogorov–Smirnov test, for the measurement time point T_1 vs T_2 : FDM sup, FDM inf, DLP sup, DLP inf, Two-sample Kolmogorov–Smirnov test, $p < 0.01$). Nevertheless, ~99% of HD values were < 1 mm and ~80% < 0.4 mm for all measurements, which according to the literature is an admissible difference and indicates that the geometry of the FVM model were printed correctly with both techniques. To compare the quality of the surfaces that provide the tactile experience during surgical planning we measured the surface roughness (SR) of the FDM and DLP printed physical models' surfaces. We chose two ROIs from both, FDM sup and DLP sup, surface meshes: one plain like and one highly curved structure, the superior vertebral endplate and the superior part of the pedicle, respectively. We found that the SR values of the surface meshes of the FDM printed model were significantly larger compared to the DLP printed model for the endplate ROI (Two-sample Kolmogorov–Smirnov test, $p \leq 0.01$), and in the case of the pedicle ROI (Two-sample Kolmogorov–Smirnov test, $p \leq 0.01$). However, the roughness values are relatively small on the entire ROI surfaces, with ~99% of the SR values being < 0.05 mm for the DLP printed model, and ~99% < 0.1 mm for FDM model in the case of the endplate. In the case of the pedicle ROI ~99% of SR values are < 0.09 mm for the DLP and for FDM model.

4.4.2. Clinical implementation of a physical model printed with FDM technology

We present a case of a 12-year-old patient suffering from congenital scoliosis due to an L.I hemivertebra. During examination, the patient complained about back pain and fatigue; the physical examination did not reveal any sensorimotor deficits. In spite of conservative treatment (physical therapy, brace for two years), the clinical and radiological signs suggested progression (COB angle 67° in coronal plane, and 90° kyphotic deformity in the sagittal plane); therefore, surgical treatment was indicated. A corpectomy and stabilization surgery from Th.IX to L.IV was planned.

The virtual model of the Th.XI-L.III vertebrae was integrated in the clinical communication via a 3DPDF document (see Materials and Methods), which provided access to its 3D content through the institutional database. Being assisted by the patient-specific 3D virtual model, the surgical team opted for a corpectomy and stabilization from Th.IX to L.IV. Our studies on FDM and DLP technologies revealed that the geometrical accuracy and surface qualities of the FDM printed models are adequate (HD, SR < 1 mm) and because its affordability, we chose to print our model with the FDM 3D printing technology. We used the physical model (1:1 scale) for surgical planning, namely, to precisely define the trajectory and angle of the transpedicular screw insertion at the Th.XII and L.II levels. During drilling, the internal grid structure of the FDM model supported the drill bit and allowed the precise

insertion of guidance titanium rods. The rods, due to their length, were protruding and indicating clearly the ideal axis of the screw insertion. As a result of the visual guidance during the operation, we were able to find the optimal axis of the screw insertion and perform the planned surgery successfully.

4.5. PART V. Affordable surgical navigation using 3D printing and FEA

4.5.1 Navigation template geometrical accuracy and performance

In this study, through a clinical case, we demonstrate a technology development process in order to create patient-specific drill guide. Based on the QCT of the patient the method not only made a virtual surgical plan with two different screw insertion orientation possible, but also made the design of drill guide safe for screw insertion at the level of the first sacral vertebra with a geometrical difficulty caused by a broken screw from previous surgery. The investment casted cobalt-chrome drill guide does not lose the geometrical properties of the pattern (3D printed drill guide model created with MSLA technology) based on the 3D scanning evaluation. To evaluate the drill guide performance a 3D printed patient-specific physical model was used. The physical model with the two drilling orientation was scanned with CT segmented and aligned to the virtual surgical plan. The drill guide provides a highly accurate screw insertion in both investigated positions. The cylinders representing the drilling axes were not perfectly colinear and coincident with the screws in the virtual surgical plan, but it did provide grade A (Gertzbein-Robbins scale) screw insertion.

4.5.2. FEA results

In the presented workflow two possible screw insertion scenarios were investigated in a patient-specific FE model by integrating the individual geometry and bone material properties based on QCT. Nine models were created for each screw insertion scenario (N=9, S1 and N=9, ALA) with increasing element numbers based on the virtual surgical plan. The FE simulation results converged above $2 \cdot 10^5$ elements for both screw insertion scenarios at ~ 5 min solve times on 2 cores. The solve time at 2 cores for the S.I orientation was higher compared to the ALA. The convergent screw insertion (S.I) is stiffer (6617.23 ± 1106.24 N/mm) compared to the divergent (ALA) insertion ($2989.07 \pm N/mm$).

4.5.3. Recommended surgical technique

Based on the FEA result the SI1 screw insertion surgical plan and drill guide position is recommended for surgical implementation. The surgical technique for the screw insertion via the developed drill guide is presented. The technique uses cannulated screws, and tip. The developed drill guide solves a support for a stainless-steel cylinder inlet to orientate the drill bit and the Kirschner -wire.

5. CONCLUSION

Based on the result of the survey research we can delineate tasks that are crucial for the further development and for the large-scale spinal application of 3D technologies. The clarification of the clinical cost-effectiveness of the technology is fundamentally requiring further clinical research projects with the active participation of spine surgeons. Spine surgeons should take part in the whole process not only as end- users but they have to be involved in the R&D steps as well. An optimal interdisciplinary work between researchers, engineers, and clinicians in order to develop and deliver new treatment possibilities through innovation can be supported by research funds but also facilitated by the active involvement of the med-tech industry. Another important task is the education and know-how delivery which must be successfully implemented through educational events.

Patient-specific computational methods provide accurate information about the unique and complex geometrical/anatomical relations due to intervertebral disc degeneration. In my thesis in Part II. the 3D geometrical change of the spinal canal and the indirect decompression effect of a minimally invasive surgical procedure (PCD) was investigated with a new, computational 3D volumetric measurement method. Significant associations with the indirect decompression and the clinical improvement have been revealed. Due to its relative simplicity we suggest the application of our measurement method for the scientific and clinical analysis of other surgical procedures based on indirect decompression effect such as anterior lumbar interbody fusion (ALIF), lateral lumbar interbody fusion (LLIF), oblique lumbar interbody fusion (OLIF), extreme lateral interbody fusion (XLIF).

Computational methods can provide accurate information about the implant construct deformation after sacrectomy, reconstructed with the „Closed Loop” technique. In part III of my thesis, I developed a method for implant deformation investigation using the postop CT scans collected over 6 years follow-up period of a patient who underwent sacrectomy and Closed Loop reconstruction. The method was able, not only to demonstrate the non-rigidity of the construct by measuring the geometry deformation over the FU but mapped the bone remodelling at the fusion site (lumbar spine-two iliac bone) as well. Significant associations with the sagittal plane deformation and the postop day were found, resulting in a forward bending tendency of the construct. Due to its relative simplicity, the application of the developed measurement method is suggested for the scientific and clinical analysis of other surgical procedures for the reconstruction of the lumbo pelvic junction after sacrectomy, and for other clinical scenarios where large construct is needed such as idiopathic or degenerative deformity corrections, grooving roods systems, etc. The data obtained via this method could be used for FEA models' validation and implant development.

Testing the accuracy of entry level (lower cost) 3D printing technologies, that are locally available on the healthcare market, is important for every clinician using such methods in surgical planning or education using 3D printed physical models.

Part IV of my thesis has proven that a more cost-effective technology is sufficiently precise enough for 3D printed physical models of the spine. If other less expensive technologies can similarly be proven to be adequate for several purposes, than the cost of 3D printing technologies can be reduced to a level that is not only acceptable for healthcare systems but will promote their widespread use.

The developed patient-specific template presented in Part V. of my thesis for pedicle screw insertion allows the surgeon to insert the screw into its optimal position. Its advantages compared to the conventional surgical navigation techniques are the relatively low cost, and the potential to reduce the intraoperative X-ray exposure and the possibility for the consideration of the patient-specific bone geometry and biomechanics. This new patient- and condition-specific approach can be widely used in revision spine surgeries or in challenging primary cases after its further clinical validations.

11.1. Publications that formed the basis of the dissertation:

1. **Eltes, P. E.**, Kiss, L., Bartos, M., Eöszé, Z., Szövérfi, Z., Varga, P. P., & Lazáry, Á. (2019). Attitude of spine surgeons towards the application of 3D technologies—a survey of AOSpine members. *Ideggyógyászati szemle*, 72(7-8), 227-235.
2. Costa, M. C., **Eltes, P.**, Lazary, A., Varga, P. P., Viceconti, M., & Dall’Ara, E. (2019). Biomechanical assessment of vertebrae with lytic metastases with subject-specific finite element models. *Journal of the mechanical behavior of biomedical materials*, 98, 268-290.
3. **P. E. Eltes**, Kiss, L., Bartos, M., Gyorgy, Z. M., Csakany, T., Bereczki, F., ... & Lazary, A. (2020). Geometrical accuracy evaluation of an affordable 3D printing technology for spine physical models. *Journal of Clinical Neuroscience*, 72, 438-446.

11.2 Publication in the field of In Silico Medicine/ Musculoskeletal modelling as co-author

1. van Rijsbergen, M., van Rietbergen, B., Barthelemy, V., **Eltes, P.**, Lazáry, Á., Lacroix, D., *Noailly J, Ho Ba Tho MC., Wilson W., Ito, K.* (2018). Comparison of patient-specific computational models vs. clinical follow-up, for adjacent segment disc degeneration and bone remodelling after spinal fusion. *PloS one*, 13(8), e0200899.
2. Dao, T. T., Pouletaut, P., Charleux, F., Lazáry, Á., **Eltes, P.**, Varga, P. P., & Tho, M. C. H. B. (2015). Multimodal medical imaging (CT and dynamic MRI) data and computer-graphics multi-physical model for the estimation of patient specific lumbar spine muscle forces. *Data & Knowledge Engineering*, 96, 3-18.
3. Castro-Mateos, I., Pozo, J. M., **Eltes, P. E.**, Del Rio, L., Lazary, A., & Frangi, A. F. (2014). 3D segmentation of annulus fibrosus and nucleus pulposus from T2-weighted magnetic resonance images. *Physics in Medicine & Biology*, 59(24), 7847.

11.3. Publication in the field of spine surgery as co-author

1. Kiss, L., Varga, P. P., Szoverfi, Z., Jakab, G., **Eltes, P. E.**, & Lazary, A. (2019). Indirect foraminal decompression and improvement in the lumbar alignment after percutaneous cement discolasty. *European Spine Journal*, 1-7.
2. Klemencsics, I., Lazary, A., Szoverfi, Z., Bozsodi, A., **Eltes, P.**, & Varga, P. P. (2016). Risk factors for surgical site infection in elective routine degenerative lumbar surgeries. *The Spine Journal*, 16(11), 1377-1383.
3. Klemencsics, I., Lazary, A., Valasek, T., Szoverfi, Z., Bozsodi, A., **Eltes, P.**, ... & Varga, P. P. (2016). Cross-cultural adaptation and validation of the hungarian version of the Core Outcome Measures Index for the back (COMI Back). *European Spine Journal*, 25(1), 257-264.
4. Szövérfi, Z., Lazary, A., Bozsódi, Á., Klemencsics, I., **Éltes, P. E.**, & Varga, P. P. (2014). Primary Spinal Tumor Mortality Score (PSTMS): a novel scoring system for predicting poor survival. *The Spine Journal*, 14(11), 2691-2700